SAR Image Formation Process and Non-stationary Errors Influence in Aircraft Motion

Su Su Yi Mon, and Fang Jiancheng

***Abstract*—On account of large amount of signal processing required in SAR imagery, the early SAR designs implemented optical processing techniques. The ground speed is biased by the inertial navigation unit drifts and to which SAR processing is extremely sensitive. It can also be recovered from the GPS technique, but this requires a GPS receiver on the ground. Another complication is that the synthesis process is made non-stationary by the nonlinearities in the aircraft motion. This is motion compensation problem. Therefore, this paper provides a fine resolution SAR image platform and finished the relationship with SAR imagery errors between the stationary and non-stationary platform to continue future motion compensation process. A new Matlab based program for SAR image formation is also developed in this paper and a few visualization enhancement features facilitates processing data and producing desired output. The SAR properties in range and azimuth directions are also described. The received echo SAR signal is described. Moreover, the simulation results and comparison would show the way of making effects on SAR image resolution related to the motion compensation.**

***Index Terms*—Synthetic Aperture Radar, Range Doppler, Motion Compensation, Image Resolution**

I. Introduction

Nowadays, Synthetic Aperture Radar (SAR) [4] [5] imaging has been widely used and has played an important role in nation and international working as a new function of radar. It can work all-time, all weather, gain high resolution image of the ground target, which enhance the ability of getting information, especially the sensing ability of war fields. To achieve high resolution, it is necessary to transmit a large bandwidth. The range resolution is inversely proportional to the RF transmitted bandwidth. SAR system works in the millimeter-wave band. Thus, a large bandwidth can be more easily transmitted because the relative bandwidth is low.

An important step in the ground processing of airborne SAR imagery is motion compensation [2] [3]. SAR depends on having accurate knowledge of the radar-target positions which leads to a requirement that the aircraft flight path be known to high precision. With reference to Figure 1, ease of processing demands that the aircraft be flown along a straight flight path for strip mapping SAR. However, since factors such as turbulence and pilot error make it impossible for an aircraft to fly along this nominal straight flight path, some motion compensation is necessary.

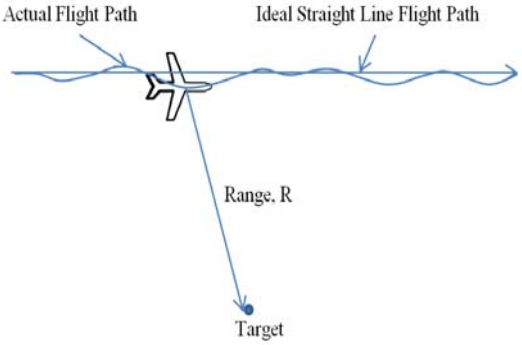

Fig. 1. Sensor – target distance on the slant range plane [9].

II. SAR Principle

SAR has some interesting properties, however, it is not known from optical sensors. These properties are as follow: SAR is an active imaging method, i.e., it provides its own illumination and, hence, is implemented of sun illumination. SAR uses microwaves that penetrate clouds and partially canopy, soil and snow. Typical wavelengths are 3cm (X-band), 6 cm (C-band), and 24cm (L-band). SAR uses polarized radiation and, therefore, can exploit polarization signatures of the imaged scatterers for obtaining more information about the scatterer's structure. SAR is a coherent imaging method. This is the prerequisite for SAR interferometry. On the other hand, this makes the radiometric interpretation of SAR images difficulty due to the appearance of speckle.

It has been mentioned that the propagation and reflection of electromagnetic waves strongly depends on its frequency. Figure 1 shows the atmospheric transmission for a wide frequency interval. SAR systems for wide area surveillance have to operate in frequency areas with minimal attenuation. Beyond the Ka-band only short range systems are realizable. Advantages of systems with a higher frequency are a reduced system size and a simplified processing. X,- C- and L-band are very common for airborne and spaceborne sensors.

The wavelength of transmitted signals plays an important role also for the reflection characteristics. A rough surface has completely different reflection behavior compared to a smooth one. However, smoothness is a property which depends on the relation of the surface structure size to the wavelength. Another feature of low frequency waves is that foliage can be penetrated thus low frequency systems are useful in some situations.

Mauscript received October 9, 2011; revised October 12, 2011.

Su Su Yi Mon is currently a Ph.D student in the school of Instrumentation Science and Opto-electronics Engineering, Beihang University, Beijing, China. (email: ssyimon@gmail.com).

Professor Fang Jiancheng is the Dean of the School of Instrumentation Science and Opto-electronics Engineering, Beihang University, Beijing, China.

III. SAR Geometry and Modes of Operation

The SAR system stores the received signals in a two-dimensional data array which is parameterized in radar position and echo signal delay which is denoted by t. As shown in Fig. 2, the antenna moves in the direction of the y-axis. Since the velocity of the radar signals is very large compared to the sensor velocity, the geometry can be assumed to be static for one transmit-receiver-cycle.

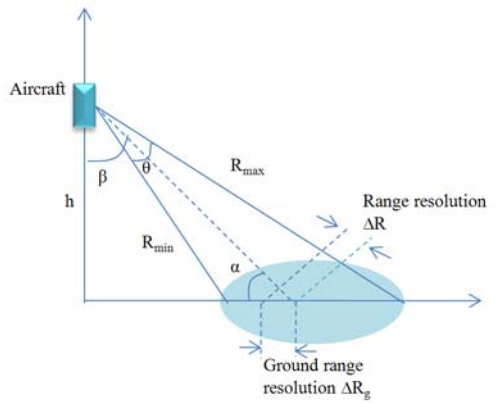

Fig. 2. Sensor – target distance on the slant range plane.

The fine resolution SAR image is mainly focus on the resolution cell of range and azimuth. The range resolution ΔR can be calculated by cτ/2 and τ is denoted as pulse width. The azimuth resolution is determined by the Doppler bandwidth of the received signal and can be computed as L/2 and L is the antenna length.

Depending upon the system's configuration, SAR sensors can acquire data in different modes. Some are totally different systems and some are just different modes of a system. The followings are some modes of SAR operation.

- Stripmap SAR
- Scan SAR
- Spotlight SAR
- Inverse SAR
- Bistatic SAR
- SAR Interferometry

IV. Geometry in Range

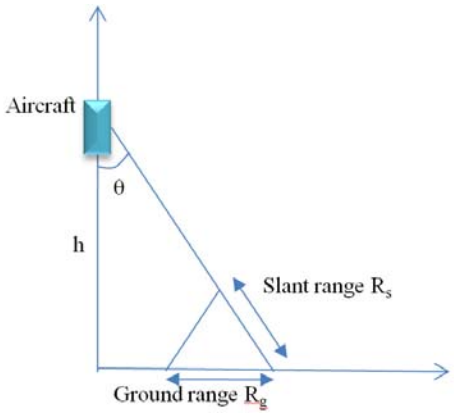

Fig. 3. Geometry in Range

SAR data are often converted from the slant range projection into the ground range one as shown in Figure 11. It is noted that SAR data in ground range projection are neither in a cartographic reference system nor geometrically corrected. The only way to correctly geocode SAR data is by applying a rigorous range-Doppler approach starting from SAR data in the original slant range geometry. Fig. 3 shows how data is acquired across a range swath. The radar beam has a certain beam width which is called the "elevation beamwidth". The beam illuminates an area on the ground between "near range" and "far range". At a certain propagation time, the pulse is transmitted as a wave front, between the two dashed lines in the Figure. The pulse expands outward in concentric spheres, at the speed of light.

V. Geometry In Azimuth

As the sensor moves along its path, pulses are transmitted and received by radar. The pulses are transmitted every "1/PRF" of a second, where PRF is Pulse Repetition Frequency. Since the sensor moves with the speed of V_s, Doppler Effect has to be taken into account. The received signal has the same waveform as the transmitted signal, but is much weaker and has a frequency shift because of sensor's moving. The shift is governed by the speed of platform. Transmitted pulses are evenly spaced. When the radar is not transmitting it receives echoes reflected back from ground surface. This is shown in Fig. 4.

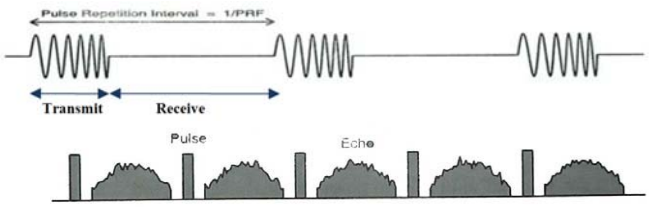

Fig. 4. Pulse transmission in Azimuth direction.

The frequency of the backscattered signal, which is registered by the antenna, depends on the relative velocity between sensor and the target. Parts of the signal, which are reflected from targets in front of the sensor, are registered with a higher than the emitted frequency, since the antenna is moving towards the target. Similarly, the registered frequency of objects that are behind the sensor is lower than the emitted frequency. In the spaceborne case the Earth's rotation and curvature causes Doppler shifts which depend on the position of the target within the imaged swath. A target at the far range has a higher radial velocity than a target closer to the sub-satellite track. Therefore, frequency shifts are range dependent.

Finally, topographic differences also have an effect on the radial velocities between sensor and targets and therefore influence the geometry in azimuth.

VI. Imaging Algorithms

As described in introduction, there are several SAR processing algorithms available, and each has its advantages and disadvantages. Some of these algorithms are:

- Chirp Scaling Algorithm
- InSAR Algorithm
- Omega-K Algorithm
- SPECAN Algorithm
- Range Doppler (RD) Algorithm

The Chirp Scaling Algorithms is not much different to Range Doppler Algorithm. The first difference is that in CSA, a Chirp Scale factor comes in to equations which basically affect the FM rate. However Chirp Scale factor is 1 for satellite SAR systems, but it plays a key role in airborne SAR systems. Second difference of CSA is that radar FM rate is modified to handle higher squints3 [12].

The Omega-K algorithm [15] can be described in five principal steps:

- Fourier transform of data
- Matched filter in range
- Matched filter in azimuth
- Stolt Mapping
- Inverse Fourier transform to find the image

The main difference is the use of position as the independent variables in each dimension. The challenge SAR processing poses is a non-separable, range-dependent point spread function. A range-dependent correlation filter could be used; however, the point spread function has a large region of support in the spatial domain and implementing such a filter requires an enormous amount of computation.

SAR can obtain high resolution images of the ground targets, and it can work for all time and all weather. Data processing of SAR is generally carried out by pulse compression. A popular algorithm for pulse compression is SPECAN algorithm which is computationally efficient but cause an undesirable range dependent scaling of the image azimuth pixel dimension. Replacing the standard Fourier transform (FT) with an appropriate chirp-z transform can achieve a constant azimuth pixel.

The RD [7] [8] processes the raw SAR data calculated from to produce the SAR image space or final image. The RDA performs matched filtering separately in the Fourier transformed range and azimuth domains. The Fourier transforms are calculated via fast Fourier transforms (FFTs) for processing time efficiency. Range cell migration correction (RCMC) is performed in the range time and azimuth frequency domain. This domain is called the range-Doppler domain and gives its name to the algorithm as performing the RCMC in this domain is the defining feature of the algorithm when compared to other SAR processing algorithms. A Flow chart of the RD algorithm is shown in Fig. 5

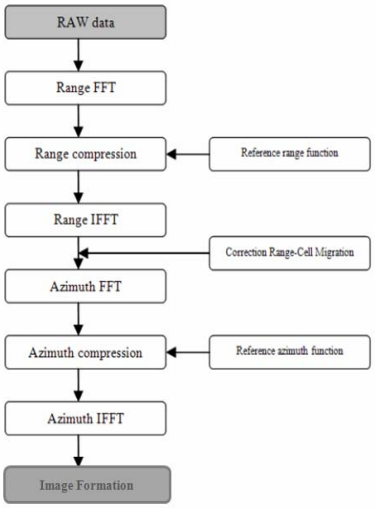

Fig. 5. RD Flow Chart

A. Raw Data

As mentioned before, data is converted to range and azimuth-frequency domain by performing Fourier Transformation on every column of data (azimuth fft). The next step is to transform data to 2D frequency domain. This is done by another Fourier transformation on the rows of data (range fft). After that range compression performs the matched filtering on every row of range samples. The matched filter $h(t)$ is designed with $h(t) = p(-t)$, where $p(t)$ is equals the transmitted signal.

$$p(t) = A_0 \operatorname{Re} ct\left(\frac{t - T_p/2}{T_p}\right)\exp\left[j2\pi f_c t + j\pi K t^2\right] \quad (1)$$

where A_0 is the amplitude of the transmitted signal and $\operatorname{Re} ct\left(\frac{t - T_p/2}{T_p}\right)$ is a rectangular gate function with T_p as the pulse duration time. The symbol f_c is the carrier frequency, and K is the LFM pulse chirp rate. (1) states that the signal $p(t)$ starts time $t = 0$ and ends at $t = T_p$.

Therefore for simplicity, we will use $a(t)$ to substitute the gate function and let $A_0 = 1$. The echo with reflection coefficient σ_i at range R_i, for i=1,2,…,I can be represented by a sum of delayed signals as:

$$s(t) = \sum_{i=0}^{I} \sigma_i a(t - \tau_i)\exp\left[j2\pi f_c (t - \tau_i) + j\pi K (t - \tau_i)^2\right] \quad (2)$$

where $\tau_i = 2R_i / c$ is the echo delay time due to the i th target. For a target located at (x_i, y_i) and with a radar position at (0,0) and assuming the radar height H=0, the delay time can be computed as follows:

$$\tau_i = \frac{2R_i}{c} = \frac{2\sqrt{x_i^2 + y_i^2}}{c} \quad (3)$$

$$R_i = \frac{c\tau_k}{2} \quad (4)$$

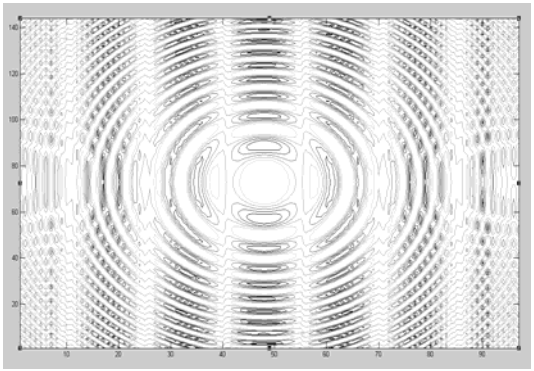

Fig. 6. Simulation results of SAR echo

The raw SAR received signal for the simulation is assumed to be of the form shown in (75. It is expressed by letting n be time index of the received and digitized LFM signal and can be obtained by removing the high carrier frequency through the quadrature demodulation process which brings the signal

to baseband [1] [15].

$$s_b(t_n) = \sum_{i=0}^{I} \sigma_i \left| a(t_n - \tau_i) \right|^2 \exp\left[-j2\pi f_{c2} \tau_i + j\pi K (t_n - \tau_i)^2 \right] \quad (5)$$

where n =0,1,2,…,N-1 and N is the total number of received range samples.

B. Range Compression

Range compression is performed on each range line of SAR data, and can be done efficiently by the use of the Fast Fourier Transform (FFT). The frequency domain range matched filter needs to be generated only once, and it is applied to each range line. The range matched filter may be computed or generated from a replica of the transmitted pulse. In addition, the range matched filter frequency response typically includes an amplitude weighting to control sidelobes in the range impulse response. The steps in range compression for each range line are Rang FFT and Rang IFFT.

C. Azimuth Compression

After range compression, the signal energy from a point target follows a trajectory in the two-dimensional SAR data that depends on the changing range delay to the target as it passes through the antenna beam. This trajectory may cross several range bins. In order to capture all the signal energy for azimuth compression, the signal energy from a point target must be aligned in a signal range bin.

Azimuth compression is a matched filtering of the azimuth signal, performed efficiently using FFT's. Note that the azimuth FFT has already been performed at this point. The azimuth FFT's were performed on blocks of data that overlap in azimuth by the matched filter length. The reason for the overlap is the throw-away after azimuth compression. Azimuth matched filter is created similar to range matched filter. It is also applied in the same way. The original formula for azimuth matched filter is:

$$h(t) = \exp\left\{ t \frac{4\pi f_0 R_0 L}{c} \right\} \quad (6)$$

The two-dimensional signal is first analyzed as a series range time signals for each azimuth bin. Each range time signal undergoes matched filtering in the range frequency/azimuth time domain through range FFTs applied to the range time signals. After each signal is transformed back into the range time/azimuth time domain, the result is the range compressed signal as the matched filtering was performed in the range frequency domain. In order to obtain azimuth compression, azimuth matched filtering must be performed. The range compressed signal is then composed into a series of signals with respect to azimuth time at different range bins. Each azimuth signal is Fourier transformed via an azimuth FFT.

VII. Simulation Parameters and Results

As in the systems parameters, SAR image processing based on RD system is implemented. Taking relevant parameter shown in Table 1 into the equations above, we get the synthetic aperture length *Ls* is 120m and Doppler frequency bandwidth is 80Hz. Besides that number of azimuth samples and time samples can be calculated as 300 and 256 respectively.

Fig.7 and Fig.8 show the complete simulation using received single point target signals. Using the parameters listed in Table I, we need to shorten the range chirp length and azimuth exposure time in order to fit the simulation into a 128×256 point array. To achieve this shortening, we have increased the range and azimuth FM rates, to keep the bandwidths the same. Reducing the radar wavelength was one parameter changed to achieve this.

TABLE I: Parameters Used in Simulation

Parameter	Symbol	Value
Wavelength	λ	0.03(m)
LFM duration	T_p	5(μs)
LFM Bandwidth	B	30(MHz)
Doppler Chirp Rate	f_{Dc}	-33.333(Hz)
Azimuth Sample Spacing	A_s	0.4m
Synthetic Aperture Length	Ls	120m
Antenna Length	L	2
Doppler Frequency Bandwidth	$BDop$	80Hz
Closet Range of Target	R_0	8000m

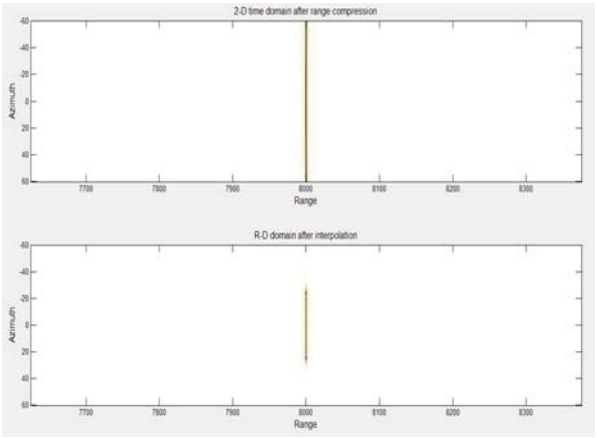

Fig. 7. Point target simulation after range compression.

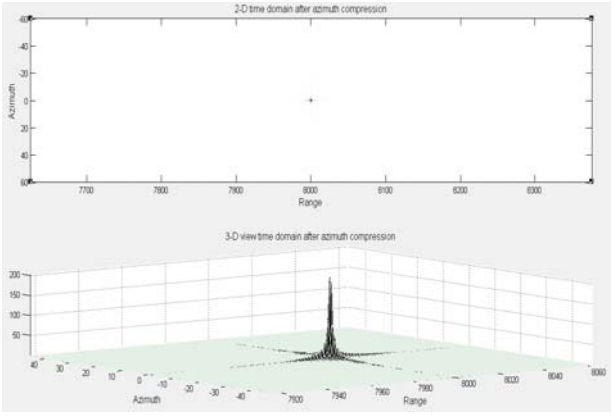

Fig. 8. Point target simulation after azimuth compression.

Accordingly by reason of the comparison between Fig. 9 (a) and (b), it is the need for aircraft motion compensation. This is primarily an issue with regard to airborne SAR, where

the aircraft flight path is subject to random disturbances due to atmospheric turbulence and airframe vibration. It is seen that the deviations that must be compensated for are very small. If phase errors are introduced, the azimuth beam forming gain is reduced. The phase errors appear in the image as a loss of resolution, a decrease in dynamic range, and an increase in noise.

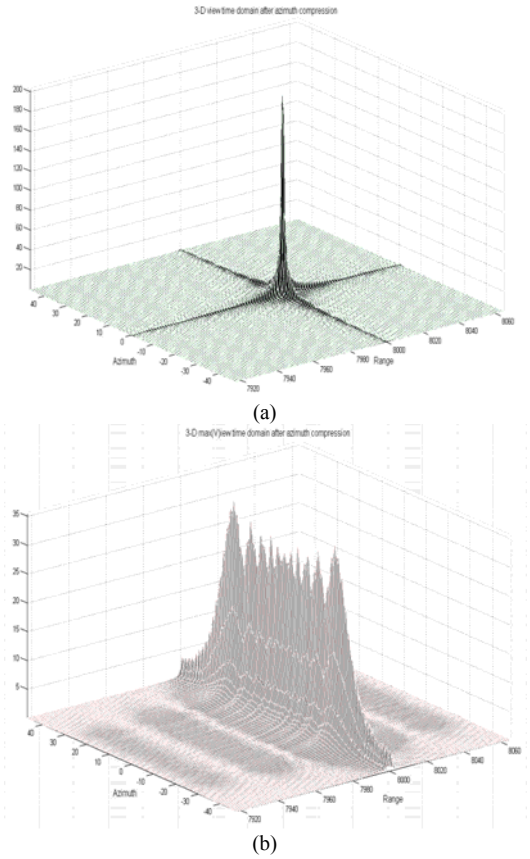

(a)

(b)

Fig. 9. Point target simulation between stationary and non-stationary state

After a careful study and analysis of RD algorithm with simulation coded on Matlab, the basic procedure is carried out for each of echo pulse range compression, and then RD domain, by interpolation to eliminate the distance of migration caused by the coupling between the distance and direction to finalize the deal with the azimuth focus, as follows.

In real time SAR system, the real time Doppler spectrum transmitted over the data link becomes necessary to carry out most of the motion compensations. Several types of radial motion should be considered when determining motion cancellation requirements. A constant aircraft velocity component in the radial vr produces a displacement of the synthetic image. For large values of vr, the displacement may exceed the antenna beamwidth, creating a dark band across the image. A constant component of radial acceleration ar produces an image azimuth distortion. For high-frequency low-amplitude sinusoidal motions, these are typical of antenna vibrations.

The method requires that one or more stationary point targets be included in the data. The phase history of each reference target is estimated for the period in which the target is in the view of the radar. The phase error, computed as the deviation from the theoretical phase function, is estimated and removed from the raw data. Unfortunately, conventional continuous phase measurement requires high signal-to-noise ratio. To increase the effective signal-to-noise ratio of the raw reference target data, the targets must be extracted after matched filtering, and the resulting data must be from inverse matched filtered. In one test data set, this phase correction method improved the SAR image resolution by fifty percent.

VIII. Conclusion

In this Paper, SAR image formation is processed using range Doppler (RD) algorithm. Based on the purpose of the SAR imaging processing, different processing algorithms have well preference. According to the principles of RD theory, the same principles apply to two dimensional FFTs , due to its cyclic nature, an FFT of length N (where N is even) consider elements 0 to N/2-1 to correspond to positive temporal or frequency samples and elements N/2 to N to correspond to negative temporal or frequency samples. This ordering scheme is not how the data is recorded, and is not particularly desirable when trying to plot the temporal or frequency samples, so the samples are often left in the original or logical sate and the data is reformatting or shifted to the FFT form prior to the FFT and then shifted back to the logical state after each implementation of the FFT or inverse FFT (iFFT).

Moreover, the measure error velocities for the near and far slant ranges, are used to calculate values for the horizontal and vertical velocity error components. These components are then fed back as correction to the acceleration inputs, with the loop time constant of several seconds. Finally, this paper concludes from the comparison of the final image formation between the constant target image and error putting to that of. Therefore, it can be concluded that motion compensation is very important for airborne SAR systems and the modified version of range Doppler algorithm to compensate motion errors is aimed as addition research to advance in future work.

Acknowledgment

The author heartily thankful to her supervisor and advisor, Prof. Fang Jiancheng and Prof.Sheng Wei from School of Instrumentation Science and Opto-electronics Engineering for their kindly helpful, suggestions related to this work. Moreover, the author would like to show her thankfulness to every single one from laboratory for their friendly kindness and helping her all the way up, especially, Associate Prof. Yu Wenbo and Mr. Wael Mohsen Ahmed Soliman, who support her, several valuable advices.

References

[1] R.Bamler, "A comparison of range-Doppler and wavenumber domain SAR focusing algorithms," *IEEE Trans. Geosci.Remote Sensing,* vol. 30, pp. 706-713, July 1992.

[2] Moreira, A.; Huang, Y. "Airborne SAR processing of highly squinted data using a chirp scaling approach with integrated motion compensation." *IEEE Trans. Geosci. Remote Sens*. vol. 32, pp. 1029-1040, 1994.

[3] I. Cumming D. Stevens and A. Gray, "Options for airborne interferometric sar motion compensation," *IEEE Trans. Geosci. Remote Sens.*, vol. 33, pp. 409–419, March 1995.
[4] I.G. Cumming., F.H. Wong., Digital Processing of Synthetic Aperture Radar Data. Artech House, 2005.
[5] M. Soumekhl., Soumekh, Synthetic Aperture Radar Signal Processing with MATLAB Algorithms. John Wiley and Sons, 1999.
[6] Ian G.Cumming, Frank H.Wong "Digital Processing of Synthetic Aperture Radar Data: Algorithms and Implementation," Beijing, Publishing House of Electronics Industry, 2007.
[7] Bassem R. Mahafza, "Radar Systems Analysis and Design using MATLAB, Chapman&Hall/CRC, Boca Raton, FL, 2000.
[8] Zaharris, Brian. Two-Dimensional Synthetic Aperture Radar Imaging and Moving Target Tracking Using the Range Doppler Algorithm Simulated in Matlab, San Luis Obispo, CA: California Polytechnic State University San Luis Obispo California, 2006.
[9] Guccione, P., Cafforio, C., "Motion Compensation Processing of Airborne SAR Data" *IEEE Trans. Geoscience and Remote Sensing Symposium,* vol. 5, pp. 1154-1157, July 2008.
[10] Soumekh, Mehrdad, "Bi-static synthetic aperture radar inversion with application in dynamic object imaging," *IEEE Trans. On Signal processing*, vol.39, pp.2044-2055. Sept 1991.
[11] Naeim Dastgir."Processing SAR data using Range Doppler and Chirp Scaling Algorithms," Royal Institute of Technology (KTH), 100 44 Stockholm, Sweden, 2007.
[12] Mehrdad. Soumekh, "Synthetic Aperture Radar Signal Processing with MATLAB Algorithms," John Wiley & Sons, Inc, New York, 1999.
[13] Xuesong Jin and Yong Li,"Study on dual-stripmap imaging algorithm for airborne circular-scanning SAR data processing," APSAR, , Oct. 2009, pp. 108-111, doi:10.1109/APSAR.2009.5374297.
[14] R.K.Raney, "AN exact wide field digital imaging algorithm," Science,vol.13, pp. 991-998, Mar. 1992,
[15] Zarko Cucej and Dusan Gleich, "Signal Processing for Synthetic Aperture Radars," in Proc. Internationl conference on Systems, signals and Image processing Press, June. 2010.

Su Su Yi Mon was born in May 1981 and has received her B.E (EC) degree in Electronics Department from Mandalay Technological University (MTU), Mandalay, Myanmar, in 2003, the M.E (EC) degree in Electronics Department from Yangon Technological University (YTU), Myanmar, in 2006. She worked as a Lecturer in Technical University, Hmaw Bi, (2006-2007) and researcher in MSMERC, Dattaw, (2007-2008) and her research interests were in the area of signal and image processing of radar system and antenna theory. She is currently a Ph.D student in Instrumentation Science and Opto-electronics Engineering at Beihang University, Beijing, China.

Prof. Fang Jiancheng was born in September 1965. He received the B.S. degree from Shandong University of Technology (now Shandong University), Jinan, China, in 1983, the M.S. degree from Xi'an Jiaotong University, Xi'an, China, in 1988, and the Ph.D. degree from Southeast University, Nanjing, China, in 1996. He is the Dean of the School of Instrumentation Science and Optoelectronics Engineering, Beijing University of Aeronautics and Astronautics, Beijing, China. He has authored or coauthored over 150 papers and four books. He has been granted 35 Chinese invention patents as the first inventor. Prof. Fang has the special appointment professorship with the title of "Cheung Kong Scholar," which has been jointly established by the Ministry of Education of China and the Li Ka Shing Foundation. He is in the first group of Principal Scientists of the National Laboratory for Aeronautics and Astronautics of China. He received the first-class National Science and Technology Progress Award of China as the third contributor in 2006, the first-class National Invention Award of China as the first inventor, and the second-class National Science and Technology Progress Award of China as the first contributor in 2007.